

ANALYTICAL APPLICATIONS OF THE J INTEGRAL*

J. G. Merkle

Oak Ridge National Laboratory
Oak Ridge, Tennessee**MASTER**

ABSTRACT

It has recently been shown by experiment that a quantity known as the J Integral may be a useful fracture criterion in the inelastic range. The mathematical definition of the J Integral is used here to derive a relationship between the conventional elastic stress concentration factor of a sharp notch and the elastic stress intensity factor for a crack of the same shape. This relationship has previously been derived only by assuming some particular shape of cracked body, but this assumption is shown to be not necessary. The same assumptions, together with Neuber's equation for the inelastic stress and strain concentration factors for a sharp notch, are used to derive a relationship between the J Integral and the parameter K_{Icd} of the Equivalent Energy Method. A graphical procedure for estimating upper and lower bounds on the full restraint value of the fracture toughness is also discussed.

* Research sponsored by the U. S. Atomic Energy Commission in support of the Heavy Section Steel Technology Program, under contract with the Union Carbide Corporation.

NOTICE

This report was prepared as an account of work sponsored by the United States Government. Neither the United States nor the United States Atomic Energy Commission, nor any of their employees, nor any of their contractors, subcontractors, or their employees, makes any warranty, express or implied, or assumes any legal liability or responsibility for the accuracy, completeness or usefulness of any information, apparatus, product or process disclosed, or represents that its use would not infringe privately owned rights.

DISTRIBUTION OF THIS DOCUMENT IS UNLIMITED

Nomenclature

A_c	Crack area, in. ²
a	Defect size, generally half-length, in.
B	Plate thickness, in.
C	Shape factor, dimensionless
c_1	Constant, in. ⁻¹
c_2	Constant, dimensionless
E	Modulus of elasticity, psi
G_c	Critical elastic strain energy release rate, in.-lb/in. ²
G_{cl}	Critical elastic strain energy release rate measured with a large specimen, in.-lb/in. ²
G_I	Elastic strain energy release rate for plane strain conditions, in.-lb/in. ²
G_{Ic}	Critical elastic strain energy release rate for plane strain conditions, in.-lb/in. ²
J	The J Integral, in.-lb/in. ²
J_c	Critical value of the J Integral, in.-lb/in. ²
J_{cs}	Critical value of the J Integral measured with a small specimen, in.-lb/in. ²
J_{Ic}	Critical value of the J Integral measured under plane strain conditions, in.-lb/in. ²
K_c	Critical value of the elastic crack tip stress intensity factor, ksi.in. ^{1/2}

K_c^*	Critical value of the elastic crack tip stress intensity factor estimated from the value of S_f^* , ksi.in. ^{1/2}
K_I	The elastic crack tip stress intensity factor, ksi.in. ^{1/2}
K_{Ic}	Critical value of the elastic crack tip stress intensity factor for plane strain conditions, ksi.in. ^{1/2}
K_{Icd}	The same as K_c^* ; the subscript d indicates the size (usually thickness) of the specimen being considered; in this report, d is sometimes represented by m, p, t or ∞ ; ksi.in. ^{1/2}
K_t	Elastic stress concentration factor, dimensionless
K_e	Actual strain concentration factor, dimensionless
K_σ	Actual stress concentration factor, dimensionless
k'	Initial slope of the curve of P/B^2 versus Δ/B , ksi
m	Thickness of a model specimen, in.
P_f	Failure load, kips
P_f^*	Pseudo-elastic failure load, kips
p	Thickness of a prototype, in.
S	Nominal stress, ksi
S_f	Actual nominal stress at failure, ksi
S_f^*	Pseudo-elastic nominal stress at failure, ksi
$s_{m,t}$	The size effect, also called the volumetric energy ratio, between the sizes m and t, dimensionless

t	Thickness, in.
U	Nominal strain energy density, ksi
V	Total potential energy, in.-kips
W	Width of a Compact Tension Specimen, in.
W_o	Strain energy density at the crack tip on the plane of crack extension, ksi
W_s	Strain energy density on the crack tip contour, ksi
x	Distance in the direction of crack extension, in.
Y	Shape factor for the Compact Tension Specimen; also sometimes denoted by $f(a/W)$; dimensionless
y	Distance perpendicular to the plane of crack extension, in.
Γ_t	The crack tip contour (not an algebraic quantity)
Δ	Displacement of the load, in.
θ	Position angle measured at the crack tip, radians
λ	Total nominal strain, in./in.
ϵ_{max}	Maximum total strain at the notch tip, in./in.
ν	Poisson's ratio, dimensionless
ρ	Notch tip radius of curvature, in.
σ_{max}	Maximum stress at the notch tip, ksi

σ_r

Stress normal to the notch tip surface, ksi

 σ_θ

Stress tangential to the notch tip surface, ksi

 σ_Y

Yield stress, ksi

Introduction

The need for measured values of the fracture toughness, K_{Ic} , for nuclear pressure vessel steels is the result of the requirement that the safety of nuclear power plants must be proven in advance, by methods of analysis that are as quantitative as possible and that agree with experimental data.¹ Current testing procedures require that the size of the specimen required to measure a valid value of K_{Ic} must increase with the square of the ratio K_{Ic}/σ_Y . This results in specimens as thick as twelve inches being required to measure a valid value of K_{Ic} for unirradiated A533-B steel at room temperature. Such thickness requirements reduce to a practical impossibility the irradiation of specimens sufficiently thick to measure the higher values of K_{Ic} required to quantitatively demonstrate the safety margins that exist for irradiated nuclear pressure vessels. Consequently, there is a need for ingenious alternate approaches to the quantitative determination of high values of fracture toughness, using small volumes of irradiated material. One approach, described by Klausnitzer and Gerscha,³ is to insert, by electron beam welding, a small irradiated crack tip element into a larger unirradiated specimen. Another approach is to rely on a theoretical relationship between the elastic-plastic load-deflection behavior of a small specimen and the elastic fracture toughness that would, or might have been, measured directly, using a much larger specimen. The latter approach is the one to be discussed in this paper.

Current Approaches to the Development of
Elastic-Plastic Fracture Analysis

In order to obtain a measure of fracture toughness from a specimen that has been fractured after gross yielding, it is first necessary to hypothesize a fracture criterion that is not based on the assumption of completely elastic behavior. To do this, it is logical to begin by making the assumption that the onset of fracture is caused by a critical condition of stress or strain being reached at or near the crack tip. If changes in transverse restraint due to gross section yielding are ignored, at least temporarily, then in addition it can be assumed that the critical condition remains the same regardless of whether the specimen fails before or after gross section yielding. Thus if an assumed critical quantity can be calculated, or measured directly, from inelastic ultimate load data obtained from a small specimen, and it can be calculated, for elastic conditions, for other geometries, then it can be used as a basis for calculating K_{Ic} . Such a quantity, known as the J Integral, was suggested by Rice⁴ as an analytical device for the inelastic range. Rice⁴ showed that the J Integral, which for a notch with a finite root radius no matter how small, has the definition

$$J = \int_{\Gamma_t} W_s dy \quad , \quad (1)$$

where Γ_t is the crack tip contour, W_s is strain energy density in ksi, and y is the distance normal to the crack plane in inches, is also equal to minus the rate of change of total potential energy with respect to crack surface area, at constant deflection, assuming nonlinear elastic behavior.

Thus,

$$J = - \frac{\partial V}{\partial A_c} \quad , \quad \Delta = \text{const} \quad , \quad (2)$$

where V is total potential energy in inch-kips, A_c is crack surface area in in.², and Δ is the displacement of the load, in inches. Clearly, Eq. (2) is a generalization of the equation for G_c , the elastic strain energy release rate. In addition, if J has a critical value at fracture, which can be denoted by J_c , then Eq. (1) gives an explicitly stated notch tip condition at fracture.

Following the reasoning developed by Rice,⁴ Begley and Landes⁵ of the Westinghouse Research Laboratories showed experimentally, with specimens of Ni Cr Mo V rotor steel and A533-B steel, that the value of J_{Ic} obtained from small specimens is substantially the same as the value of G_{Ic} obtained previously from much larger specimens. In other words,

$$J_{cs} = G_{cl} = \frac{K_c^2}{E}, \quad (3)$$

where the subscripts s and l indicate small and large specimen sizes, respectively. Landes and Begley⁶ also presented evidence indicating that J_{Ic} is independent of geometry.

Another generalization, for inelastic conditions, of the elastic equations used to calculate K_{Ic} has been proposed by Witt and Mager.⁷ For a Compact Tension Specimen which fails after the onset of gross yielding, a fracture toughness parameter, K_{Icd} , is defined by the equation

$$K_{Icd} = \frac{P_f^* Y}{B \sqrt{W}}. \quad (4)$$

In Eq. (4), P_f^* is the load at a point on the extended initial tangent to the actual load deflection curve which defines a pseudo-elastic load deflection curve the area under which is the same as the area under the actual load deflection curve at maximum load. Y is the elastically calculated nondimensional shape factor, sometimes denoted² by the symbol $f(a/W)$;

B is the specimen thickness, in inches; and W is the specimen width, in inches. The elastic equation for K_{Ic} , is identical in form to Eq. (4). The subscript d in the term K_{Icd} refers to the thickness of the specimen tested. The subscript I, as used by Witt and Mager,⁷ implies the opening mode of crack extension, but does not necessarily imply plane strain. Witt and Mager⁷ found that values of K_{Icd} , obtained with one-inch-thick Compact Tension Specimens of A533-B, Class 1, steel up to 50°F, match previously measured values of K_{Ic} obtained with specimens up to twelve inches thick, as shown in Figure 1. Thus, although the parameter K_{Icd} , as originally defined, appears to have no explicit meaning in terms of notch tip conditions, it has been shown to have the correct value when the correct value was already known. Thus, it is of interest to ask the question, "Does K_{Icd} have any explicit meaning in terms of notch tip conditions?" in order to evaluate its physical significance. The strategy adopted for answering this question was to begin with the equation for the J Integral, which does have an explicit meaning in terms of notch tip conditions, as given by Eq. (1), and, by a series of assumptions, to derive an expression identical to Eq. (4), thus answering the question affirmatively.

Derivation of the Irwin-Neuber Equation

Before applying the J Integral to an inelastic analysis, it will be applied first to the derivation of an important existing elastic equation relating the stress concentration factor of a sharp notch to the stress intensity factor for a crack of the same shape. The derivation to be presented here is important because it demonstrates the reasonableness of the assumptions to be used subsequently for an inelastic analysis, and because the elastic equation being derived has previously been derived only by assuming some specific overall geometry (see, for instance, ref. 8).

Since J is a generalization⁴ of G , it follows that, for plane strain elastic conditions,

$$\lim_{\rho \rightarrow 0} J = G_I, \quad (5)$$

where ρ is the notch root radius in inches. Combining Eqs. (1) and (5) gives

$$\lim_{\rho \rightarrow 0} \int_{\Gamma_t} W_s dy = G_I \quad (6)$$

If the crack tip configuration is assumed to be the arc of a semicircle, as shown in Fig. 2, and it is assumed that

$$W_s = W_0 \cos \theta, \quad (7)$$

where W_0 is the strain energy density at the point on the crack tip for which $\theta = 0^\circ$, then combining Eq. (6) and (7) gives

$$G_I = \lim_{\rho \rightarrow 0} \frac{W_0}{\rho} \int_{-\rho}^{\rho} x dy = \lim_{\rho \rightarrow 0} \frac{\pi}{2} W_0 \rho \quad (8)$$

On the crack tip contour, for elastic plane strain conditions, $\epsilon_z = 0$ and $\sigma_r = 0$, where σ_r is the stress normal to the crack surface. Consequently,

$$W_s = \frac{\sigma_\theta \epsilon_\theta}{2} = \frac{\sigma_\theta^2 (1 - \nu^2)}{2E}, \quad (9)$$

where σ_θ and ϵ_θ are the stress and the strain, respectively, tangential to the crack tip contour. For $\theta = 0^\circ$, $W_s = W_0$ and

$$W_0 = \frac{(K_t S)^2 (1 - \nu^2)}{2E}, \quad (10)$$

where K_t is the elastic stress concentration factor and S is the nominal stress. Substituting Eq. (10) into Eq. (8) and rearranging gives

$$\frac{EG_I}{(1 - \nu^2)} = \lim_{\rho \rightarrow 0} \frac{(K_t S)^2 \pi \rho}{4} \quad (11)$$

Since

$$\frac{EG_I}{(1 - \nu^2)} = K_I^2, \quad (12)$$

substituting Eq. (12) into Eq. (11) and taking the square roots of both sides gives

$$K_I = \lim_{\rho \rightarrow 0} \frac{1}{2} K_t S \sqrt{\pi \rho} \quad (13)$$

Equation (13), referred to here as the Irwin-Neuber equation,^{9,10} has already been extremely useful in the field of fracture mechanics. It has been used to derive stress intensity factor solutions when the corresponding stress concentration factor solutions were already known.¹¹ It should be noted that an assumption similar to, but not identical to, Eq. (7) has been used by Rice¹² to estimate the maximum strain at the tip of a notch, but Eq. (13) did not result.

A Relationship Between the J Integral and
the Parameter K_{Icd}

For an inelastic analysis, combining Eqs. (1) and (7), and again assuming a semicircular notch tip configuration, gives

$$J = \frac{\pi}{2} W_0 \rho, \quad (14)$$

which is a generalization of Eq. (3) without taking the limit as ρ approaches zero. Still assuming plane strain,

$$W_o = \int_0^{\epsilon_{\max}} \sigma_{\max} d\epsilon_{\max} , \quad (15)$$

where σ_{\max} and ϵ_{\max} are the maximum stress and the maximum strain, respectively, at the tip of the notch. In order to evaluate the right hand side of Eq. (15), it will be assumed that both the nominal and the notch tip stress-strain curves can be represented by equations of the form

$$\text{stress} = \text{constant} \times (\text{strain})^n . \quad (16)$$

Applying Eq. (16) to Eq. (15) thus gives

$$W_o = \frac{\sigma_{\max} \epsilon_{\max}}{1 + n} . \quad (17)$$

The actual stress and strain concentration factors are defined by the equations

$$\sigma_{\max} = K_{\sigma} S , \quad (18)$$

and

$$\epsilon_{\max} = K_{\epsilon} \lambda . \quad (19)$$

According to an analysis developed by Neuber,¹⁴ the quantity $(K_{\sigma} K_{\epsilon})$ remains constant even after yielding, and can be estimated from the equation

$$K_{\sigma} K_{\epsilon} = K_t^2 . \quad (20)$$

Neuber's original analysis¹⁴ was for in-plane shear loading, but subsequent studies by Van Buren,¹⁵ and by Gowda and Topper,¹⁶ have supported the use of Eq. (20), at least as an approximation, for other modes of loading. Therefore, substituting Eqs. (18) and (19) into Eq. (17), and using Eq. (20) gives

$$W_o = K_t^2 \frac{S\lambda}{1+n} \quad (21)$$

From Eq. (16), it also follows that

$$\frac{S\lambda}{1+n} = \int_0^\lambda S d\lambda = U \quad (22)$$

where U is the nominal strain energy density at the location of the flaw, in ksi. Combining Eqs. (21) and (22) gives

$$W_o = K_t^2 U \quad (23)$$

and combining Eqs. (23) and (14) then gives

$$J = \frac{K_t^2 U}{2} \pi r \quad (24)$$

Equation (23) expresses the basic physical relationship implied by this analysis, namely, the proportionality between the maximum strain energy density at the crack tip and the nominal strain energy density.

The elastic stress concentration factor, K_t , can be evaluated by recognizing that Eq. (13) is actually a good approximation whenever the ratio of notch depth to root radius is large. Thus, combining Eq. (13), without the limit notation,

with the basic expression for the stress intensity factor, which is

$$K_I = CS \sqrt{\pi a} , \quad (25)$$

gives

$$K_t = 2C \sqrt{\frac{a}{p}} . \quad (26)$$

Substituting Eq. (26) into Eq. (24) eliminates the unknown root radius and gives

$$J = (2\pi C^2 a)U , \quad (27)$$

Thus, the value of the J Integral is approximately proportional to the product of the crack size and the nominal strain energy density. If J has a constant value at fracture, then the product of U times a must be constant at fracture.

By substitution, Eq. (27) can be rewritten in a form identical to the equation for K_I , Eq. (25). Assuming the validity of Eq. (3), then at fracture

$$J_c = G_c = \frac{K_c^2}{E} = (2\pi C^2 a)U , \quad (28)$$

where the subscript I implying plane strain has been set aside pending experimental verification. The quantity U can be written as

$$U = \frac{(S_f^*)^2}{2E} , \quad (29)$$

where S_f^* defines the end point of a pseudo-elastic stress strain curve, the area under which is the same as the area under the actual $S - \lambda$ curve at maximum load, as shown in Fig. 3. Substituting Eq. (29) into Eq. (28) then leads to

$$K_c^* = CS_f^* \sqrt{\pi a} , \quad (30)$$

where K_c^* is an estimate of K_c based on S_f^* . Equation (30) is identical in form to both Eq. (25) for K_{Ic} , and to Witt and Mager's⁷ expression for K_{Icd} in terms of the nominal stress.

An expression applicable to the Compact Tension Specimen, and identical in form to Eq. (4), can now be derived. The first step is to define a normalized load-displacement curve that has an initial slope equal to E , the elastic modulus. The normalized load can be arbitrarily defined by the equation

$$S = \frac{P}{B^2} \quad (31)$$

Then, if the initial slope of the curve of P/B^2 versus Δ/B is k' , the normalized displacement will be defined by the equation

$$\lambda = \frac{k'}{E} \left(\frac{\Delta}{B} \right) \quad (32)$$

It is also necessary to assume that K_σ and K_ϵ remain constant during loading, and that Eq. (23) therefore remains valid.

For elastic conditions, Eq. (13) can be written, without the limit notations, as

$$K_{Ic} = \frac{1}{2} K_t S_f \sqrt{\pi p} \quad (33)$$

It follows from Eqs. (30) and (33) that

$$K_c^* = \frac{1}{2} K_t S_f^* \sqrt{\pi p} \quad (34)$$

For elastic conditions,²

$$K_{Ic} = \frac{P_f Y}{B \sqrt{W}} \quad (35)$$

Combining Eqs. (31), (33), and (35) gives

$$K_t = \frac{2BY}{\sqrt{W\pi p}} \quad (36)$$

Finally, combining Eqs. (34) and (36) gives

$$K_c^* = \frac{P_f^* Y}{B \sqrt{W}} \quad (37)$$

which is identical to Eq. (4).

Noting that

$$K_c^* = K_{Icd}^* \quad (38)$$

it follows that an approximate relationship between the J Integral and the parameter K_{Icd} does exist, subject to the limitations of deformation theory.

The above derivation should not be interpreted as a general proof that the gross load-deflection curve always controls the fracture process, beyond the elastic range. This hypothesis can be disproven by considering an edge cracked, eccentrically loaded, elastic-ideally plastic tensile bar with the crack on the side of the minimum strain. Deformation theory definitely does not apply to this specimen, because shortly after yielding occurs on the side of the maximum strain, the stress and strain on the other side (the cracked side) can begin to decrease, before yielding occurs there. A calculation of K_{Icd} for this specimen would be meaningless.

A Graphical Procedure for Estimating Upper and Lower Bounds
on the Fracture Toughness

In applying Eq. (4), Witt and Mager⁷ found that the calculated values of K_{Icd} , for A533-B steel, either remained constant or increased as the specimen size increased as shown in Figure 4. Assuming this to be the case. Witt and Mager¹⁷ proposed a calculational procedure for finding upper and lower bounds on the fracture toughness that would be obtained from an infinitely large specimen. If two geometrically similar specimens are each tested to their maximum load, then from Eqs. (29), (30), and (38),

$$\left(\frac{K_{Ict}}{K_{Icm}} \right)^2 = \frac{a_t U_t}{a_m U_m} = \frac{t}{m} \cdot \frac{U_t}{U_m}, \quad (39)$$

where the subscripts m and t denote the model size and some other size, respectively. Witt and Mager¹⁷ used the definition

$$s_{m,t} = \frac{U_m}{U_t}, \quad (40)$$

where $s_{m,t}$ is termed the size effect, or the volumetric energy ratio, between the sizes m and t. Combining Eqs. (39) and (40), and inverting, gives

$$\left(\frac{K_{Icm}}{K_{Ict}} \right)^2 = s_{m,t} \left(\frac{m}{t} \right). \quad (41)$$

For determining a lower bound, Witt and Mager¹⁷ assumed that

$$K_{Ict} = K_{Icp} \quad , \quad t \geq p, \quad (42)$$

where p represents the size of a prototype, and $p > m$.

For determining an upper bound, Witt and Mager¹⁷ assumed that

$$s_{m,t} = c_2 + c_1 t \quad , \quad (43)$$

where the constants c_2 and c_1 are determined by the values of K_{Icm} and K_{Icp} . For $t = m$,

$$c_2 + c_1 m = 1 \quad . \quad (44)$$

For $t = p$, using Eq. (41),

$$c_2 + c_1 t = s_{m,t} = \left(\frac{p}{m}\right) \left(\frac{K_{Icm}}{K_{Icp}}\right)^2 \quad . \quad (45)$$

Solving Eqs. (44) and (45) for c_1 and c_2 gives

$$c_1 = \frac{\left(\frac{p}{m}\right) \left(\frac{K_{Icm}}{K_{Icp}}\right)^2 - 1}{p - m} \quad , \quad (46)$$

and

$$c_2 = 1 - c_1 m \quad . \quad (47)$$

Combining Eqs. (41) and (43) gives

$$\left(\frac{K_{Icm}}{K_{Ict}}\right)^2 = (c_2 + c_1 t) \left(\frac{m}{t}\right) = (c_1 m) + (c_2 m) \frac{1}{t} \quad . \quad (48)$$

Equation (48) implies that if Eq. (43) is assumed, then the quantity

$(K_{Icm}/K_{Ict})^2$ will be a linear function of $1/t$. Therefore, on a plot of

$(K_{Icm}/K_{Ict})^2$ versus $1/t$, as shown in Figure 5, the upper bound value of

K_{Ict} is determined by the intercept of a straight line through the points

corresponding to $t = m$ and $t = p$ with the vertical axis, providing that the

curve is concave upward. The value of the upper bound is given by

$$\left(\frac{K_{Icm}}{K_{Ic\infty}}\right)^2 = c_1^m = \frac{\left(\frac{p}{m}\right)\left(\frac{K_{Icm}}{K_{Icp}}\right)^2 - 1}{\left(\frac{p}{m} - 1\right)}, \quad (49)$$

so that

$$K_{Ic\infty} = K_{Icm} \sqrt{\frac{\frac{p}{m} - 1}{\left(\frac{p}{m}\right)\left(\frac{K_{Icm}}{K_{Icp}}\right)^2 - 1}} \quad (50)$$

In addition, if similitude holds at fracture, for some range of thickness, then, from Eq. (40),

$$s_{m,t} = 1, \quad (51)$$

and substituting Eq. (51) into Eq. (41) gives

$$\left(\frac{K_{Icm}}{K_{Ict}}\right)^2 = \frac{m}{t}. \quad (52)$$

According to Eq. (52), the condition of similitude at fracture is represented by a straight line through the origin, in the type of plot shown in Fig. 5.

A plot of $(K_{Icm}/K_{Ict})^2$ versus $1/t$ for A533-B steel, at 100°F, 200°F and 550°F is shown in Fig. 6. This plot is based on the data shown in Fig. 4. The curves all show a tendency to be concave downward instead of concave upward. Thus, the upper bound values increase instead of decrease as p increases, for a fixed value of m , and the existence of an asymptotic value of K_{Ict} is not clearly established, at least at these temperatures. However, since K_{Ict} does increase as t increases, a value of K_{Icp} is, as assumed, a lower bound value for all thicknesses equal to or greater than p , for this material.

Discussion and Conclusions

An approximate relationship between the J Integral and the parameter K_{Icd} of the equivalent energy method has been derived. The assumptions of a semicircular notch tip configuration and the strain energy density on the notch tip varying with $\cos \theta$ were shown to be reasonable assumptions by using them to derive the Irwin-Neuber equation, Eq. (13). The use of Neuber's inelastic stress and strain concentration factor equation, Eq. (20), may be incompletely justified theoretically, but it has enough experimental justification to warrant its use, at least on an interim basis. This equation should be further investigated theoretically. Existing data are such that the upper and lower bound values of fracture toughness do not always converge at the higher temperatures. This phenomenon also needs further study. The lower bound hypothesis is thus far confirmed by the experimental data for A533-B steel.

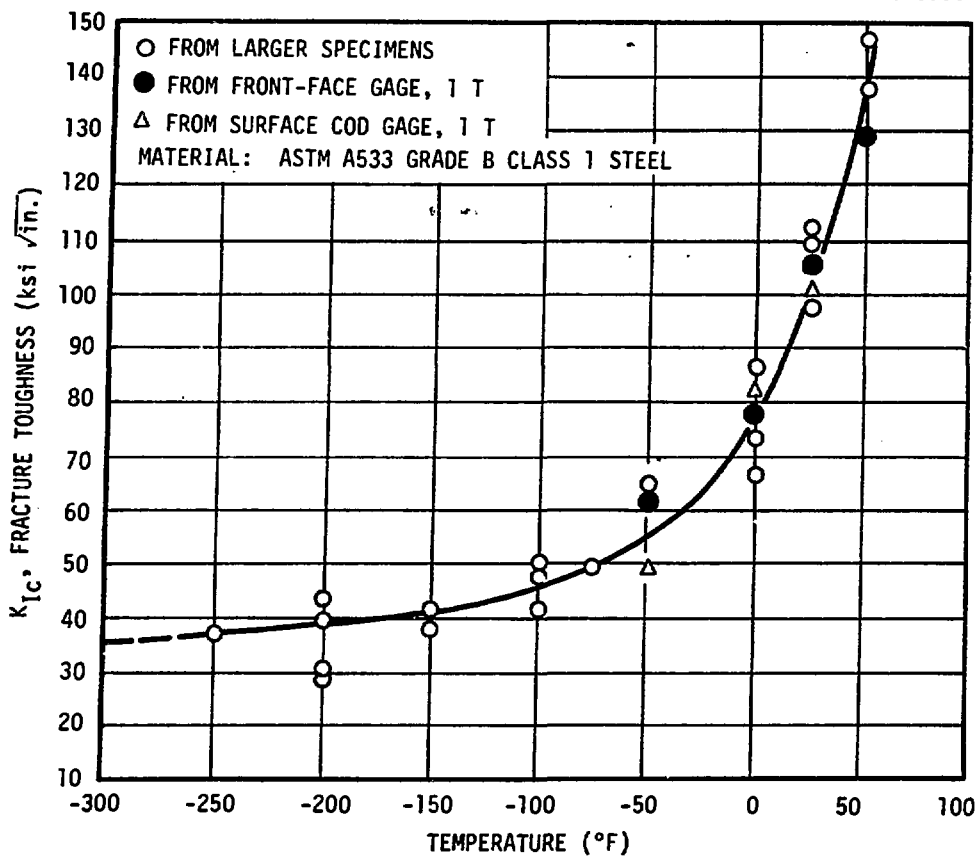
References

1. J. G. Merkle, "Fracture Safety Analysis Concepts for Nuclear Pressure Vessels, Considering the Effects of Irradiation," *Journal of Basic Engineering*, ASME, 93 (2), 1971, pp. 265-273.
2. "Tentative Method of Test for Plane-Strain Fracture Toughness of Metallic Materials," ASTM E 399-70T.
3. E. Klausnitzer and A. Gerscha, "Development of Electron-Beam Welded CT Specimens for Fracture Toughness Measurements with a Small Amount of Original Material," Paper No. 8, presented at the HSST Program Information Meeting, Oak Ridge National Laboratory, Oak Ridge, Tennessee, April 25-26, 1972.
4. J. R. Rice, "Mathematical Analysis in the Mechanics of Fracture," Chapter 3 in Volume 2 of Fracture, An Advanced Treatise, H. Liebowitz, editor, Academic Press, 1968.
5. J. A. Begley and J. D. Landes, "The J Integral as a Failure Criterion," presented at the Fifth National Symposium on Fracture Mechanics, University of Illinois, Urbana, Illinois, August 31-September 2, 1971.
6. J. D. Landes and J. A. Begley, "The Effect of Specimen Geometry on J_{Ic} ," presented at the Fifth National Symposium on Fracture Mechanics, University of Illinois, Urbana, Illinois, August 31-September 2, 1971.
7. F. J. Witt and T. R. Mager, "Fracture Toughness K_{Ic} Values at Temperatures up to 550°F for ASTM A533 Grade B, Class 1 Steel," *Nuclear Engineering and Design*, 17(1), pp. 91-102, August 1971.
8. P. C. Paris and F. Erdogan, "A Critical Analysis of Crack Propagation Laws," *Journal of Basic Engineering*, ASME, pp. 528-534, December 1963.
9. G. R. Irwin, "Fracture Mechanics," pp. 557-594 in "Structural Mechanics: Proceedings of the First Symposium on Naval Structural Mechanics," Pergamon Press, 1960.
10. G. R. Irwin et al., "Basic Aspects of Crack Growth and Fracture," NRL Report 6598, U. S. Naval Research Laboratory, Washington, D. C., November 21, 1967.
11. P. C. Paris and G. C. Sih, "Stress Analysis of Cracks," pp. 30-83 in "Fracture Toughness Testing and Its Applications," ASTM STP 381, 1965.
12. J. R. Rice, "A Path Independent Integral and the Approximate Analysis of Strain Concentration by Notches and Cracks," *Journal of Applied Mechanics*, ASME, pp. 379-386, June 1968.

13. J. G. Merkle, "An Engineering Approach to Multiaxial Plasticity," ORNL 4138, Oak Ridge National Laboratory, Oak Ridge, Tennessee, July 1967.
14. H. Neuber, "Theory of Stress Concentration for Shear-Strained Prismatical Bodies with Arbitrary Nonlinear Stress-Strain Law," Journal of Applied Mechanics, ASME, pp. 544-550, December 1961.
15. W. Van Buren, "Stress Concentration Factors by Neuber's Leading Function Method," Research Report 67-1D7-BTLPV-R2, Westinghouse Research Laboratories, Pittsburgh, Pennsylvania, August 14, 1967.
16. C. V. B. Gowda and T. H. Topper, "On the Relation Between Stress and Strain-Concentration Factors in Notched Members in Plane Stress," Journal of Applied Mechanics, ASME, pp. 77-84, March 1970.
17. F. J. Witt and T. R. Mager, "A Procedure for Determining Bounding Values on Fracture Toughness K_{Ic} at Any Temperature," presented at the Fifth National Symposium on Fracture Mechanics, University of Illinois, Urbana, Illinois, August 31-September 2, 1971.

Figure Captions

- Fig. 1. Comparison of K_{Ic} and K_{Ic1} Values up to 50°F (longitudinal direction).
- Fig. 2. Crack Tip Configuration Assumed for Analysis.
- Fig. 3. Diagram Defining S_f^* .
- Fig. 4. Variation of K_{Icd} as a Function of Temperature and Thickness, for A533-B Steel.
- Fig. 5. Schematic Example of Graphical Determination of Upper and Lower Bounds on Fracture Toughness.
- Fig. 6. Curves for Graphically Determining Bounding Values of Fracture Toughness for A533-B Steel.



COMPARISON OF K_{Ic} AND K_{Ic1} VALUES UP TO 50°F.

Figure 1

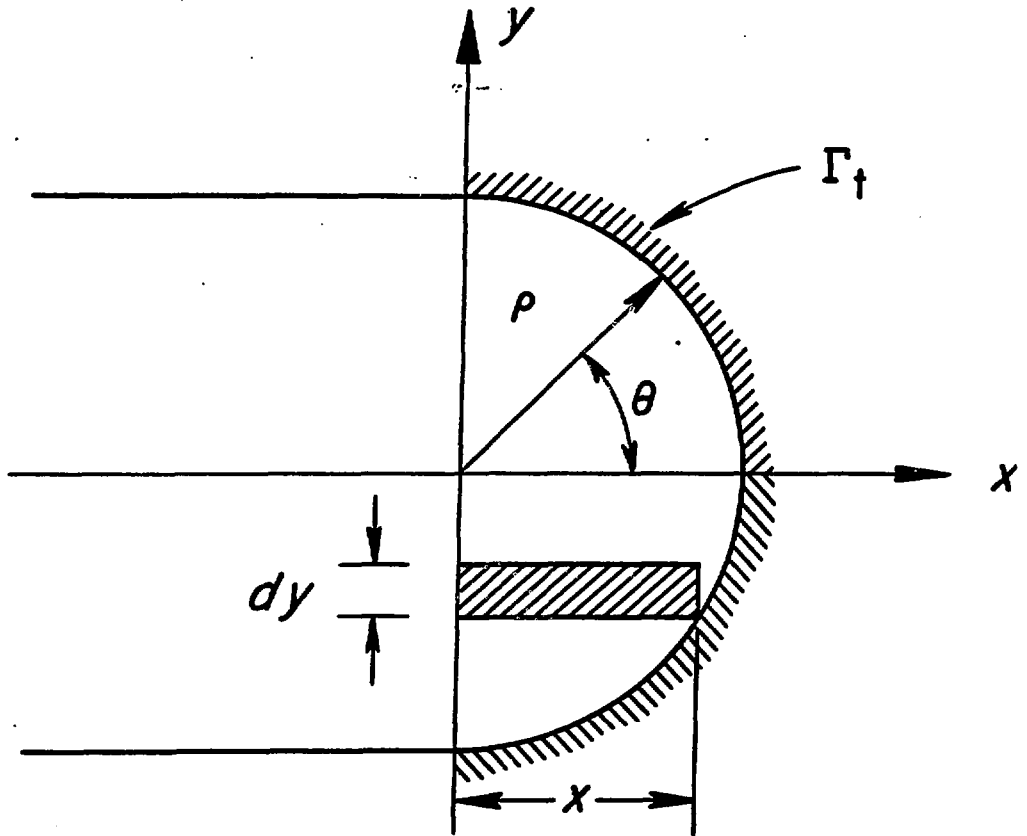


Figure 2

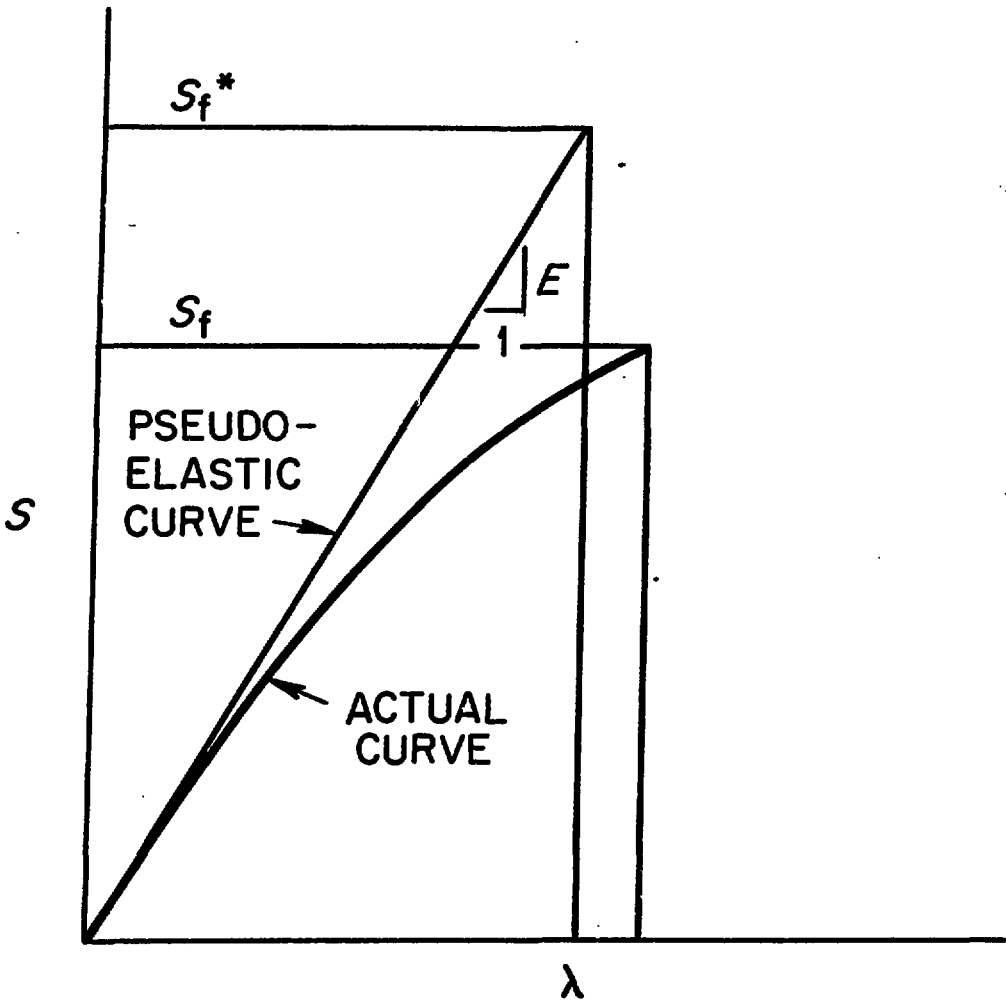
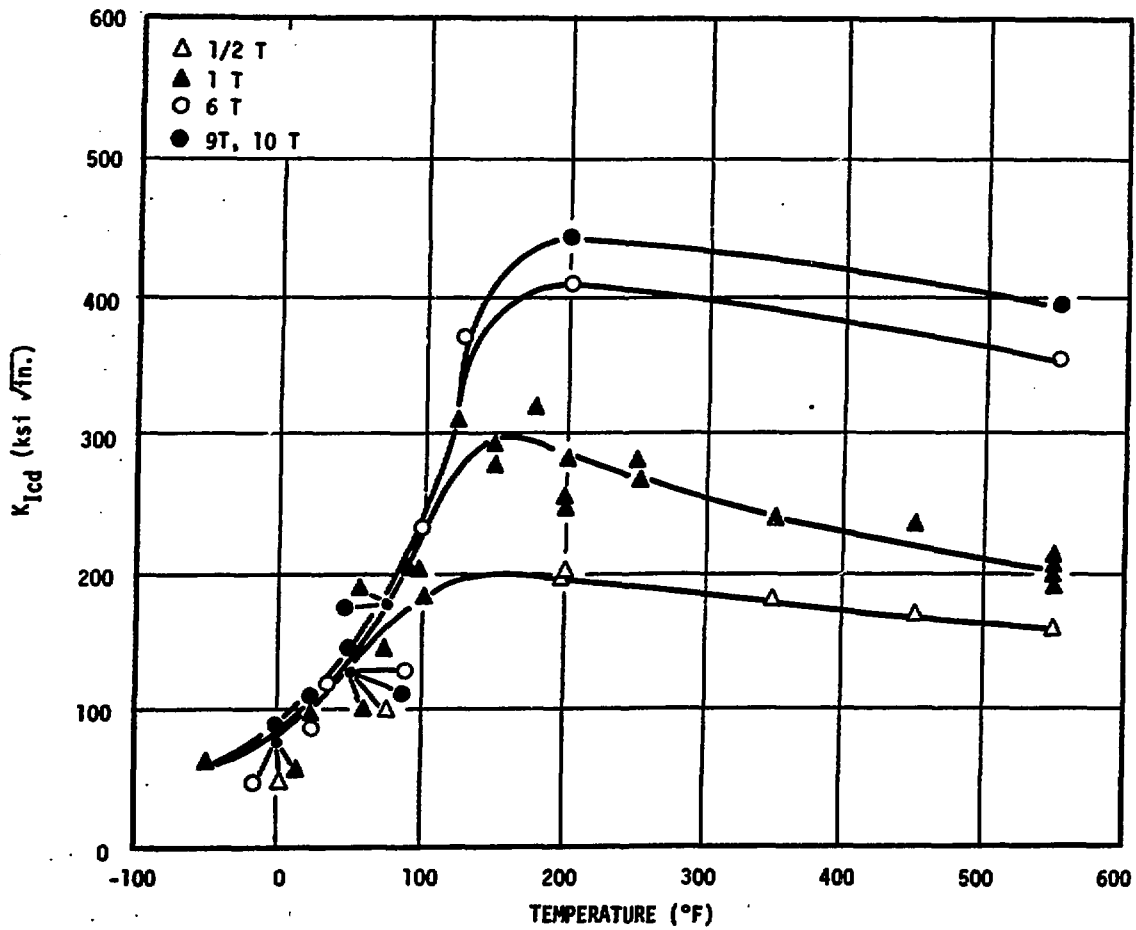


Figure 3



VARIATION OF K_{Icd} AS A FUNCTION OF TEMPERATURE AND THICKNESS

Figure 4

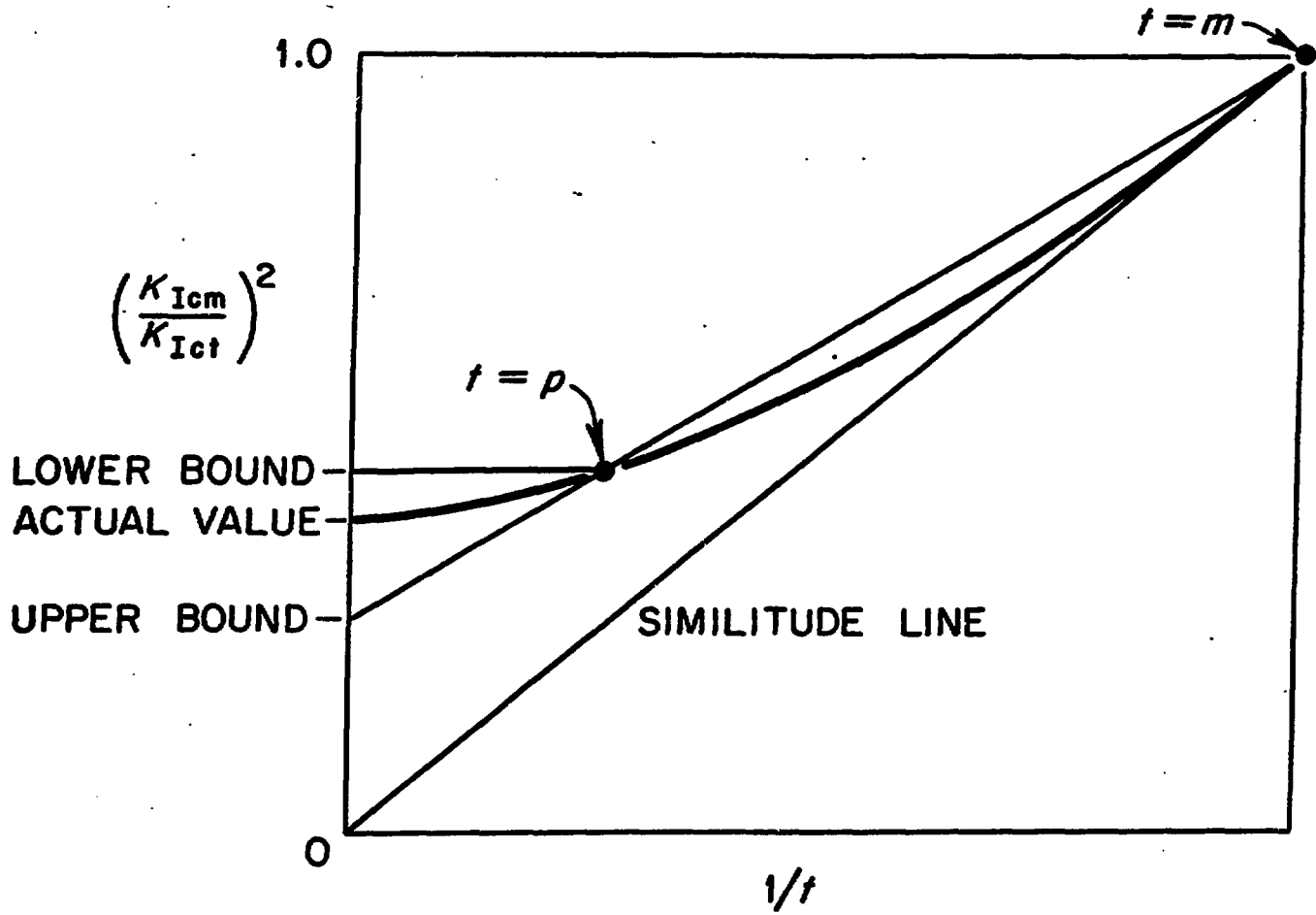


Figure 5

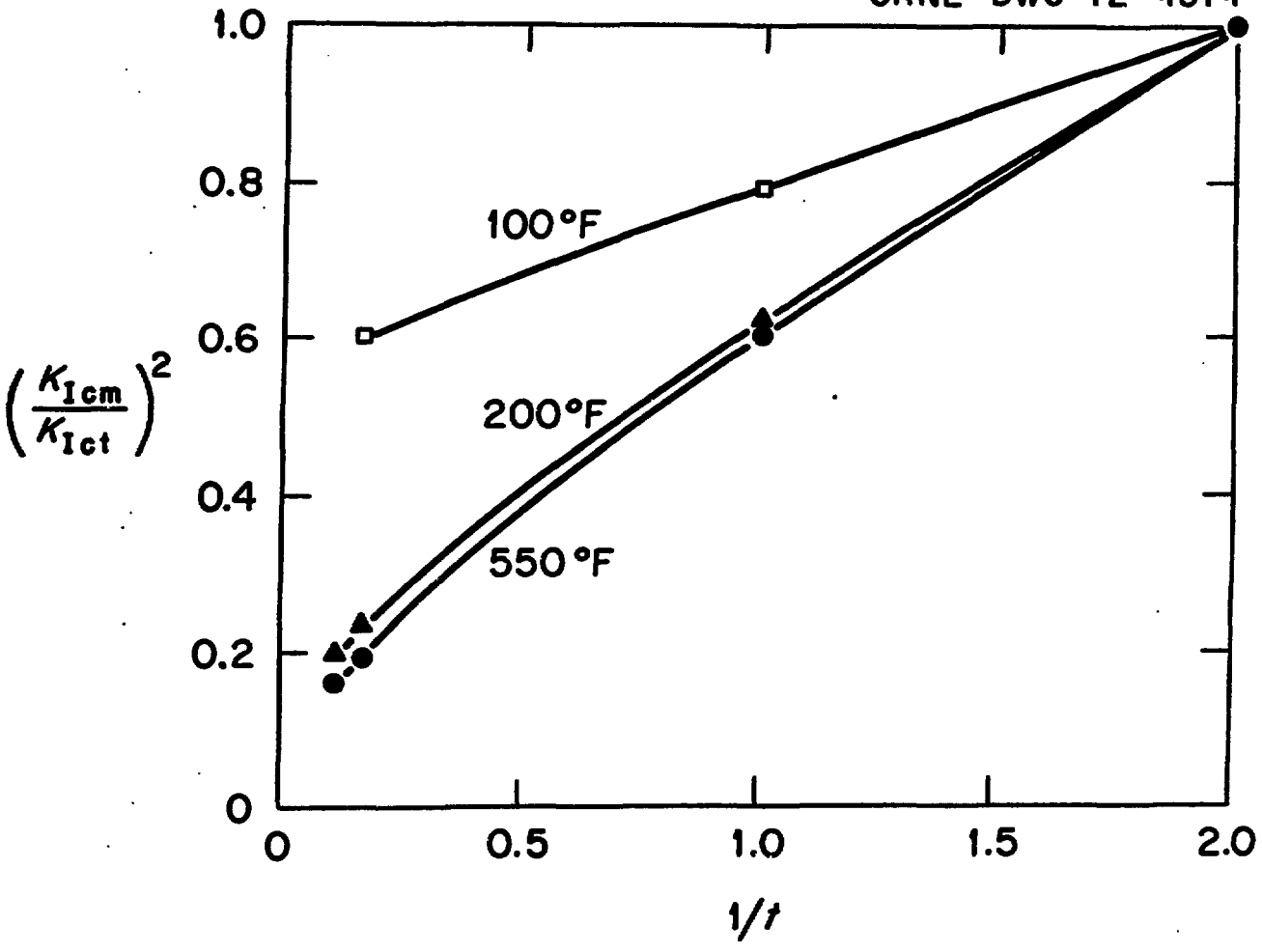


Figure 6